LRP 477/93 June 1993

AN EXPERIMENTAL STUDY OF THE HARMONICS GENERATED DURING ALFVEN WAVE HEATING IN TCA

G.G. Borg, J.B. Lister, S. Dalla Piazza,
and Y. Martin

accepted for publication in
NUCLEAR FUSION

AN EXPERIMENTAL STUDY OF THE HARMONICS GENERATED DURING ALFVEN WAVE HEATING IN TCA

G.G. Borg, J.B. Lister, S. Dalla Piazza and Y. Martin

Centre de Recherches en Physique des plasmas
Association Euratom - Confédération Suisse
Ecole Polytechnique Fédérale de Lausanne
21, Av. des Bains, CH- 1007 Lausanne, Switzerland

ABSTRACT - During plasma excitation by high power Alfven waves in TCA, signals at harmonics of the generator frequency are observed in the plasma scrape-off layer. In this paper we report experimental investigations of the sheath effect and the excitation efficiency and dispersion properties of these harmonics. The results indicate that the harmonics arise either directly or indirectly through the driven Alfven waves and not the sheath effect at the exciting antenna. The RF ion saturation current is observed to have a non-negligible peak amplitude in comparison to the time averaged ion saturation current and may provide evidence of non-linear evolution of the driven Alfven waves.

1 INTRODUCTION

Most modelling of radiofrequency (RF) wave-coupling to plasmas is simplified to exclude non-linear effects. In experiments, non-linearities are difficult to observe directly in the amplitudes and phases of the fundamental or driven waves because the plasma parameters and wave-coupling may change with RF power. Any simple non-linearity however, such as wave-steepening or amplitude saturation due to the sheath effect will generate signals at (integer) harmonics of the generator frequency. Detecting these harmonics provides a direct and unmistakable method of determining the presence of significant non-linearities, provided the excited spectrum is pure.

Harmonics of the generator frequency have been observed in experiments in the Ion Cyclotron Range of Frequencies (ICRF). Certain experiments [1,2] indicate that these harmonics are a result of the sheath effect, wherein a RF Langmuir current flows from the plasma scrape-off layer (SOL) to either the exciting antenna directly or its Faraday shield or protection limiter. RF oscillations in the SOL space potential or temperature may also drive such an RF sheath current in any conducting object in contact with the SOL; even if the object is passive and not excited directly by the RF generator. The experimental results however suggest that the harmonics originate from the region of the excited antenna, are comparable in amplitude to the fundamental, saturate in amplitude at low power and propagate in the plasma as electrostatic waves [1,2].

In ICRF, parametric decay instabilties (PDI) have been observed which result in signals whose frequencies are not necessarily integer multiples of the generator frequency. Although the PDI signals have much lower amplitude than the generator signal and its harmonics (40 dB lower is typical), they are much better documented [1-3]. In AWH, the PDI, if they exist, would have to have much lower amplitude than the harmonics.

In this paper we report the first observations of harmonics in Alfven wave heating (AWH). As in the ICRF, the harmonics in AWH have significant amplitude with respect to the fundamental and may therefore affect transport and lead to parasitic energy deposition. We aim to determine what causes the harmonics: whether they result from the sheath effect as in the ICRF or whether they are due to a more fundamental process which accompanies plasma excitation by high power Alfven waves. The results may be related to the plasma global response to AWH which is dominated by a large density rise. The density rise has made bulk heating effects of any kind difficult to discern [4].

2 EXPERIMENTAL ARRANGEMENT

In TCA there are four pairs of top and bottom antennas equally spaced toroidally. These permit antenna phasings with toroidal mode numbers N = 1, 2 and 4 and poloidal mode numbers M = 0 and 1 [5]. Experiments were performed at both 2 and 2.5 MHz with f_{ci} = 11 MHz. The experimental layout is shown in Fig. 1. TCA has a minor, major radius of 0.18 m, 0.60 m respectively and for standard plasma conditions the toroidal field was 1.5 T and the plasma current, $I_p < 130$ kA.

During these experiments we could choose to excite any combination of the eight antennas. Antenna pairs (3,7) and (4,8) were unshielded and antenna pairs (1,5) and (2,6) were electrostatically shielded [4]. A study of the effects of electrostatic screens on the plasma SOL and global response to AWH has already been presented [4]. In earlier experiments results were also obtained in which antenna pair (2,6) was shielded by a complete ceramic screen.

The wave magnetic or b-field was detected by unshielded differential magnetic probes located in the SOL. The ion saturation current was detected by a radially movable Langmuir probe. Their locations are shown in Fig. 1. The sheath current flowing from the antenna to the SOL was measured by subtracting the antenna currents detected by Rogowski coils installed on each terminal of antennas 1,2 and 3. In this paper we define the active sheath current as that which flows directly from an antenna driven by an applied antenna voltage and the passive sheath current as that which flows in an object immersed in the SOL as a result of oscillations in the plasma space potential, density or temperature and not as a result of direct excitation by the generator. The passive sheath current was monitored by measuring the sheath current flowing in an unexcited antenna. Since all antennas have an identical geometry, the active and passive sheath current amplitudes could be compared directly. Measurements of the parasitic power deposited by the active sheath current at the antenna-SOL interface was presented in [4].

3 EXPERIMENTAL RESULTS

3.1 The General Characteristics of the Harmonics

In Fig. 2, we show the poloidal b_θ-field traces of the fundamental or first harmonic, f_0 = 2.5 MHz and the second harmonic f_1 = 5 MHz for four phasings (N,M) of the antennas and with a similar antenna current in each case. The peaks are due to resonances of the discrete Alfvén wave (DAW) and coincide with peaks in the antenna loading [5]. A set of dispersion curves for the DAWs shown in Fig. 4 of [5] indicates how predictable the DAW frequencies are. We note from Fig. 2 that the DAW spectrum versus density is remarkably similar for f_0 as for f_1 with a DAW resonance appearing in the harmonic trace whenever there is a resonance in the fundamental. This important result remains true for the higher order harmonics; observations were made up to the fourth harmonic. The amplitude of f_1 in the **b**-field is generally between 2 and 10 times lower than f_0. These properties are shared by the harmonics observed on the probe floating potential and the ion saturation current. We also note that the toroidal component of the harmonic **b**-field was usually less than 20% of the corresponding harmonic poloidal component. At the fundamental, these components had similar amplitudes.

It is a well established result [5] that coupling to Alfven waves is more efficient for M=1 than for M=0. A comparison of the (1,1) trace and the (1,0) trace in Fig.2 shows not only that this is true at f_0 as expected, but that the harmonic f_1 also has a proportionately lower amplitude for M=0 than for M=1. This result would be difficult to explain in terms of the sheath effect at the exciting antenna because the antenna voltages are similar in each case.

In Fig. 3, we provide evidence that the (2,1) resonance at the second harmonic f_1 is not a DAW. In the top frame we show the density of the fundamental (2,1) resonance as a function of toroidal magnetic field. The curve is a calculation of the density versus magnetic field at which the (2,1) Alfven resonance layer (ARL) [5] enters the plasma. The calculation includes finite frequency effects [5] and is valid for a cylindrical plasma with a uniform magnetic field (taken to be the on axis field in TCA), I_p = 45 kA and Deuterium filling gas. We conclude that, despite the simplistic calculation, especially approaching the cyclotron frequency, the fundamental DAW dispersion behaves as expected. In the bottom frame, we plot the ratio of the density of the second harmonic to the fundamental resonance versus

magnetic field. The error bars are indicative of the density width of each resonance. The curve is the calculated ratio from the same cylindrical theory assuming that the harmonic has mode numbers (N,M) = (4,2). These mode numbers must be assumed if the f_1 DAW is to have a frequency near that of the f_0 DAW. If one doubles the frequency from f_0 to f_1 then one must also double the parallel wave vector given by $(N + M/q(r))/R$ where $q(r)$ is the safety factor and R the major radius in order to satisfy the Alfven wave dispersion relation in the low frequency limit [5]. We conclude that the density at which the harmonic resonance occurs corresponds to that of the fundamental DAW at 2.5 MHz and not to that of a DAW at the frequency of f_1 (= 5 MHz).

An experiment was also performed in which the density was swept through the resonant density of the fundamental (2,1) DAW at 5 MHz. No corresponding DAW was found for this density at f_1=5 MHz during excitation at fundamental f_0=2.5 MHz. From Fig. 2 there is however some evidence of resonances with small amplitudes at f_1 that do not coincide with any resonance at f_0.

Measurements were also made of the amplitude and phase of the harmonic background or continuum signals during experiments in which the RF power was 100% modulated at about 100 Hz. Analogous phase evolutions as a function of time were observed on all the harmonics as a new ARL entered the plasma [5]. This indicates that a similar non-linear mechanism to that which produces the DAW resonance harmonics is also dominant in the continua between the resonances. The amplitude variations versus instantaneous delivered power however were highly complex. Depending on the **b**-field component, harmonic and position in the spectrum, amplitude threshold as well as saturation effects can occur. The fundamental however never saturates. Some typical data are shown in Fig. 4 for the first three harmonics f_0, f_1 and f_2 of b_θ during a linear rise of the central density and excitation with shielded antenna pairs (1,5) and (2,6).

Finally we note that similar traces are observed, even at low power, if only one antenna pair is excited and that shielding the antenna has no qualitative effect on these results. From this section we conclude that the harmonics have similar dispersion properties and antenna excitation efficiencies to the fundamental Alfven spectrum as opposed to the spectrum at the respective harmonic frequencies.

3.2 An Experimental Study of the Sheath Effect

In this section, we consider the contention that the harmonics are due to either the active sheath current, the sheath current to the exciting antenna Faraday shield/protection limiter or the passive sheath current drawn by unexcited conducting objects in the SOL. We will assume, similar to the view of plasma wave excitation by an antenna, that if the harmonics are excited by the sheath effect, then a sheath current containing these harmonics must flow in the plasma [2a]. In fact, in [2b] it has been demonstrated that the harmonics generated during plasma wave excitation by an electrostatic plate antenna in the ICRF are proportional to the harmonic components of the sheath current drawn by the antenna. Because in our experiment the harmonic resonances are not DAWs, the results of this section do not depend on whether the harmonics are considered to be the direct fields of the sheath current in the plasma or waves launched by the sheath current.

In Fig. 5 from top to bottom are shown experimental traces of the first harmonic sheath current $I_f(0)$ and second harmonic $I_f(1)$, measured on unshielded antenna 3 and the first harmonic wave magnetic field, $b_\theta(0)$ and second harmonic $b_\theta(1)$ measured on the top **b**-probe.These were measured a) during excitation of antenna pair (3,7), b) antenna pair (4,8) and c) antenna pair (1,5). The sheath current measured in case a) is therefore the active sheath current, whereas in cases b) and c) it is the passive sheath current detected by antenna 3. At first sight, the b_θ data in Fig. 5 appear to be of poor quality; the first harmonic (2,1) DAW is not a single resonance but a cluster of two or more resonances. Perusal of the second harmonic traces however reveals that the fine structure is mimicked in every detail, as discussed later.

The most important result is that screens completely eliminate the active sheath current [4]. From Figs. 5a) and 5c) however, the harmonics launched by shielded and unshielded antennas have qualitatively similar amplitude and spectral properties. We conclude that the harmonics are not excited by the active sheath current, although we cannot preclude a minor contribution to the continuum or background signal due to this current.

Traces 5a) confirm this contention. Both $I_f(0)$ and $I_f(1)$ have a featureless temporal structure which follows the antenna terminal voltage. In addition, the sheath current at any point along the antenna is in phase with the antenna potential at that point [4].

The power deposited by the sheath current must therefore have a featureless temporal structure. The time evolution of the sheath current and the power it deposits is not correlated with that of the DAW spectrum. This is different to the power radiated at the fundamental. The power calcualted from $VI\cos\phi$, where V is the antenna voltage, I the antenna current and ϕ their phase difference leads to an antenna loading which is correlated with the Alfven spectrum.

The data of Fig. 5a) and 5c) also indicate that the harmonics are not excited by a sheath effect at the exciting antenna shield either. The harmonics in b_θ are more closely correlated with the first harmonic b_θ than with whether or not the antenna is shielded. Exciting an antenna with a ceramic shield also produced the harmonics.

The sheath current driven passively in the matching circuitry of an unexcited antenna, just like the RF component of the ion saturation current and floating potential [4], follows the Alfven spectrum. From Figs. 5b) and 5c) it does not depend on excitation by shielded or unshielded antennas. From its magnitude and temporal evolution, the passive sheath current is driven by fluctuations in the SOL parameters and is not entirely the return path of the active sheath current. The total effect of the passive sheath currents taken over the plasma periphery may easily be greater than that of the active sheath current by itself because it may flow in unexcited antennas, limiters and perhaps even the vessel wall. We must therefore consider the hypothesis that the harmonics are generated by the passive sheath current. This is at best an indirect excitation mechanism because the passive sheath current is itself excited by the SOL Alfven wavefields. To test it would require disconnection of all passive objects in the SOL. Disconnection of antenna pairs (3,7) and (4,8) during excitation of (1,5) failed to produce an observable effect on the harmonics. The interpretation is complicated because no information on the total reduction in the passive sheath current is obtainable. In the next section we investigate another mechanism by which the SOL wavefields might excite harmonics.

3.3 An Experimental Study of the RF Ion Saturation Current

In Fig. 6 we show typical traces of the time evolutions of the central line averaged density, the time averaged ion saturation current as measured by a Langmuir probe in the SOL and the antenna loading during (2,1) excitation. AWH causes a significant perturbation of the ion saturation current in the continuum and an even

larger effect during the passage of the DAW. The time averaged SOL density calculated from the ion saturation current may either increase or decrease with time at the application of RF depending on the exact radial location with respect to the antenna [6]. The time averaged probe floating potential varies significantly with the Alfven spectrum and may drop to as much as -60 V [6]. The RF potential has a similar peak amplitude. These amplitude variations are not large enough to perturb the ion saturation current measurement. In fact, the time evolution of the time averaged floating potential and ion saturation are not similar [6].

Observations with a bandwidth from dc - 20 MHz revealed that, during the continua, the peak to peak RF ion saturation current fluctuations could be > 50% of the time averaged ion saturation current. Traces of the amplitude and phase of the ion saturation current for the first three harmonics are shown in Fig. 7 for excitation with antenna pair (2,6) shielded by a ceramic screen. In the phase traces the central line averaged density is also shown. The correspondence between the time evolutions of the amplitude and the phase is much more obvious for the ion saturation current than for the **b**-fields. From f_0 to f_2 the contrast between the resonances and the background continuum increases with the order of the harmonic and the phase jumps at the resonances are directly proportional to the order of the harmonic. These effects are indicative of a simple non-linearity as can be seen mathematically by expanding a non-linear function of $Aexpj(\omega t + \phi)$ in a Taylor series. The time evolutions of the phases of the harmonics are almost identical but for a scaling factor equal to the order of the harmonic. One interesting discrepancy to this rule is the rapid decrease in the phase just after the start of AWH and due to the rise of the density which sweeps the spectrum. Here the slope of the phase versus time becomes steeper than expected from the order of the harmonic.

In Fig. 8a we show radial profiles of the first two harmonics of the ion saturation current in the SOL. These results indicate that the large RF modulation and the harmonics may extend into the plasma. Measurements of phase versus radius obtained during the density rise to obtain evidence for propagating waves was made difficult by inadequate shot to shot reproducibilty. In Fig. 8b we show that the ion saturation current harmonics do in fact saturate with increasing RF antenna voltage (and hence current). Unlike the case of the **b**-field, even the fundamental saturates.

4. DISCUSSION

In this paper, we have shown that the harmonics observed duing AWH cannot arise from the sheath effect at the exciting antenna central conductor. Experimental observations also indicate that the harmonics are unaffected by antenna shielding.This is quite different to the case in the ICRF. We have been unable however to exclude the passive sheath current as a cause of the harmonics.

The phases of the harmonics of the ion saturation current are proportional to their order. These harmonics therefore either arise from the same parasitic origin as the fundamental or through its non-linear evolution. Moreover, if the ion saturation current does represent an RF density perturbation, then the passive sheath current alone cannot be its cause. If the observed passive sheath current density to a single unexcited antenna is assumed to flow uniformly to the whole vessel surface in TCA, it could not deplete the SOL density in a half cycle at 2.5 MHz. The observed passive sheath current could however partly explain the observed **b**-field harmonics. The **b**-field probes may also be sensisitve to some direct magnetic or electric pick-up arising from the sheath effect at the ceramic tube containing the probes.

The fact that the ion saturation current measurements could imply a large RF density perturbation in the SOL during AWH has interesting physical implications. The temporal evolution of the traces of Fig. 7 suggests that the perturbations are Alfven waves. For low densities such that $\omega < k_{//} v_A$, where $k_{//}$ is the parallel wavevector and v_A the Alfven speed and for the TCA SOL [7] where $\beta < m_e/m_i$, the surface quasielectrostatic wave (SQEW) is expected to propagate [8] and may be excited by either fast wave mode conversion or directly by the antenna. Because of its expected low damping rate in the TCA SOL, the SQEW could have a density perturbation of large enough amplitude to produce harmonics. A computational study of simultaneous direct and mode conversion excitation of this wave has not yet been performed. Such a wave could also cause significant particle transport if it propagates in a defined direction. The rapid decrease in phase in Fig. 7 produced by the density rise at the onset of the RF pulse may be indicative of such a propagating wave.

ACKOWLEDGEMENTS

The authors would like to acknowledge the collaboration of the TCA team.
This work was funded by the Fonds National Suisse de la Recherche Scientifique.

REFERENCES

[1] VAN OOST, G., VAN NIEUWENHOVE, R., KOCH, R., et.al. "ICRF/Edge Physics Research o TEXTOR". Fusion Engineering and Design **12** (1990) 148.

[2a] VAN NIEUWENHOVE, R. and VAN OOST, G. Plas. Phys. and Contr. Fus. **34** (1992) 525.

[2b] SKIFF, F. N., WONG, K. L. and ONO, M. Phys. Fluids **27** (1984) 2205.

[3] VAN NIEUWENHOVE, R., VAN OOST,G., NOTERDAEME J.-M et. al. Nucl. Fusion **28** (1988) 1603.

[4] BORG, G. G., JOYE, B. Nucl. Fusion **32** (1992) 801.

[5] COLLINS, G. A., HOFMANN, F., JOYE, B. et. al. Phys. Fluids **29** (1986) 2260.

[6] MARTIN, Y. and HOLLENSTEIN CH.. J. Nucl. Mater. **162-164** (1989) 270.

[7] HOFMANN, F., HOLLENSTEIN, Ch., JOYE, B. et. al. J. Nucl. Mater. **121** (1984) 22.

[8] VACLAVIK, J and APPERT, K. Nucl. Fusion, **31** (1991) 1945.

Figure Captions

Fig. 1 Experimental arrangement showing the locations of the electrostatically screened antennas. As can be seen, each TCA antenna consists of 6 current straps aligned in the poloidal direction.

FIg. 2 Fundamental f_0 (left column) and harmonic f_1 (right column) for different antenna phasings (N,M). The numbers in the bottom left of the frames indicate the ranges of the measured magnetic fields.

Fig. 3 Comparison of the experimental dispersion of the fundamental and harmonic DAW resonances with the theory for DAWs.

Fig. 4 Some typical data showing the first three harmonics, f_0, f_1 and f_2 of b_θ during 100% power modulation, a linear rise of the central density and excitation with shielded antenna pairs (1,5) and (2,6). The real and imaginary parts as designated correspond to the cosine and sine outputs of a quadrature detector based on a balanced mixer.

Fig. 5 From top to bottom are shown the fundamental sheath current $I_f(0)$ and harmonic $I_f(1)$ and the poloiodal **b**-field component fundamental $b_\theta(0)$ and harmonic $b_\theta(1)$ during excitation of;
a) Antenna pair (3,7).
b) Antenna pair (4,8).
c) Antenna pair (1,5).

Fig. 6 Typical traces of central line-averaged density, SOL time averaged density and antenna loading for (2,1) excitation.

Fig. 7 Traces of the amplitude and phase of the RF ion saturation curreents f_0, f_1 and f_2.

Fig. 8 a) Radial profiles of the f_0 and f_1 RF ion saturation curents in the SOL.
b) Amplitude of the f_0 and f_1 RF ion saturation currents versus RF antenna voltage.

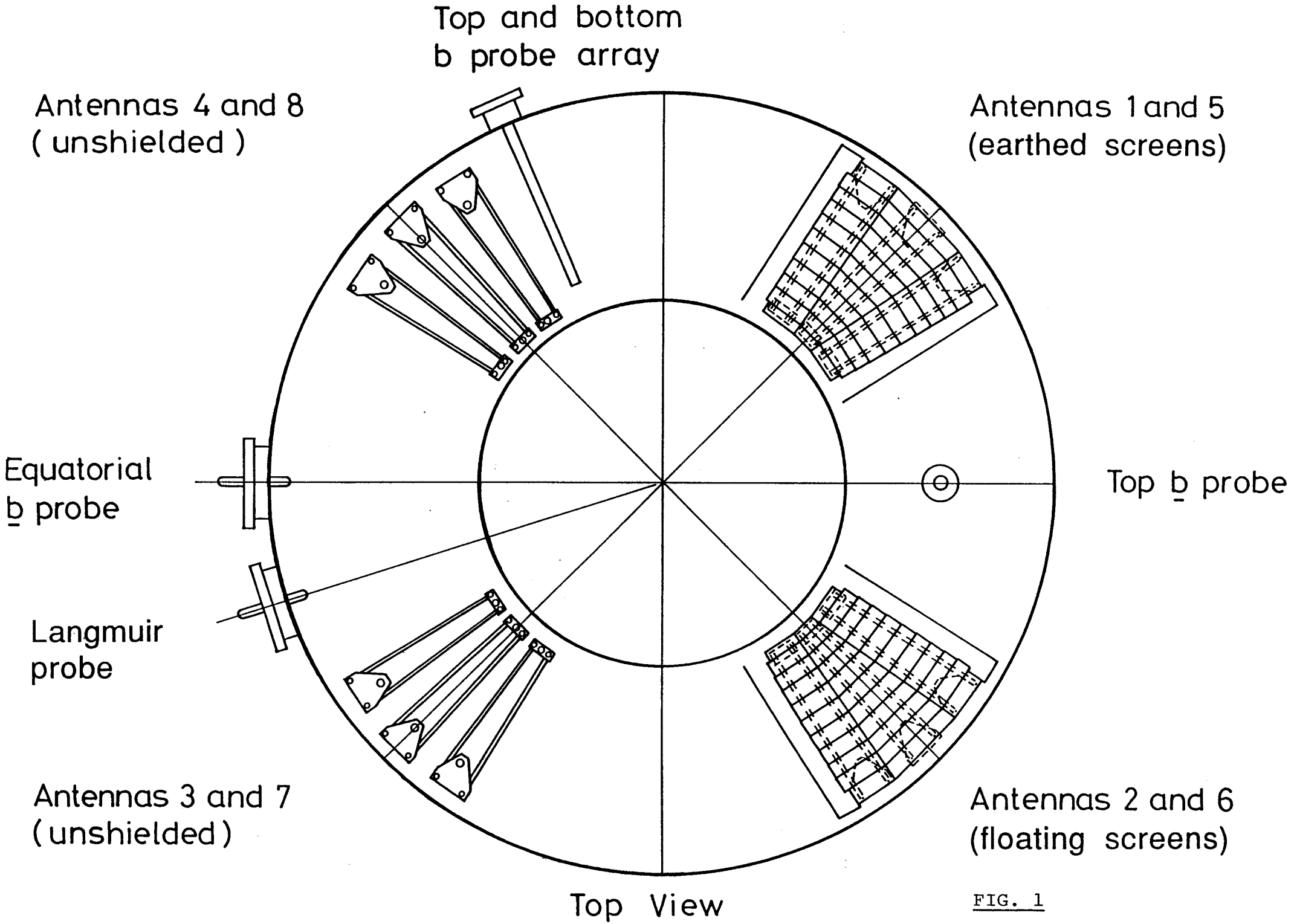
Top and bottom
b probe array
Antennas 4 and 8
(unshielded)
Antennas 1 and 5
(earthed screens)
Equatorial
b probe
Top b probe
Langmuir
probe
Antennas 3 and 7
(unshielded)
Antennas 2 and 6
(floating screens)
Top View

FIG. 1

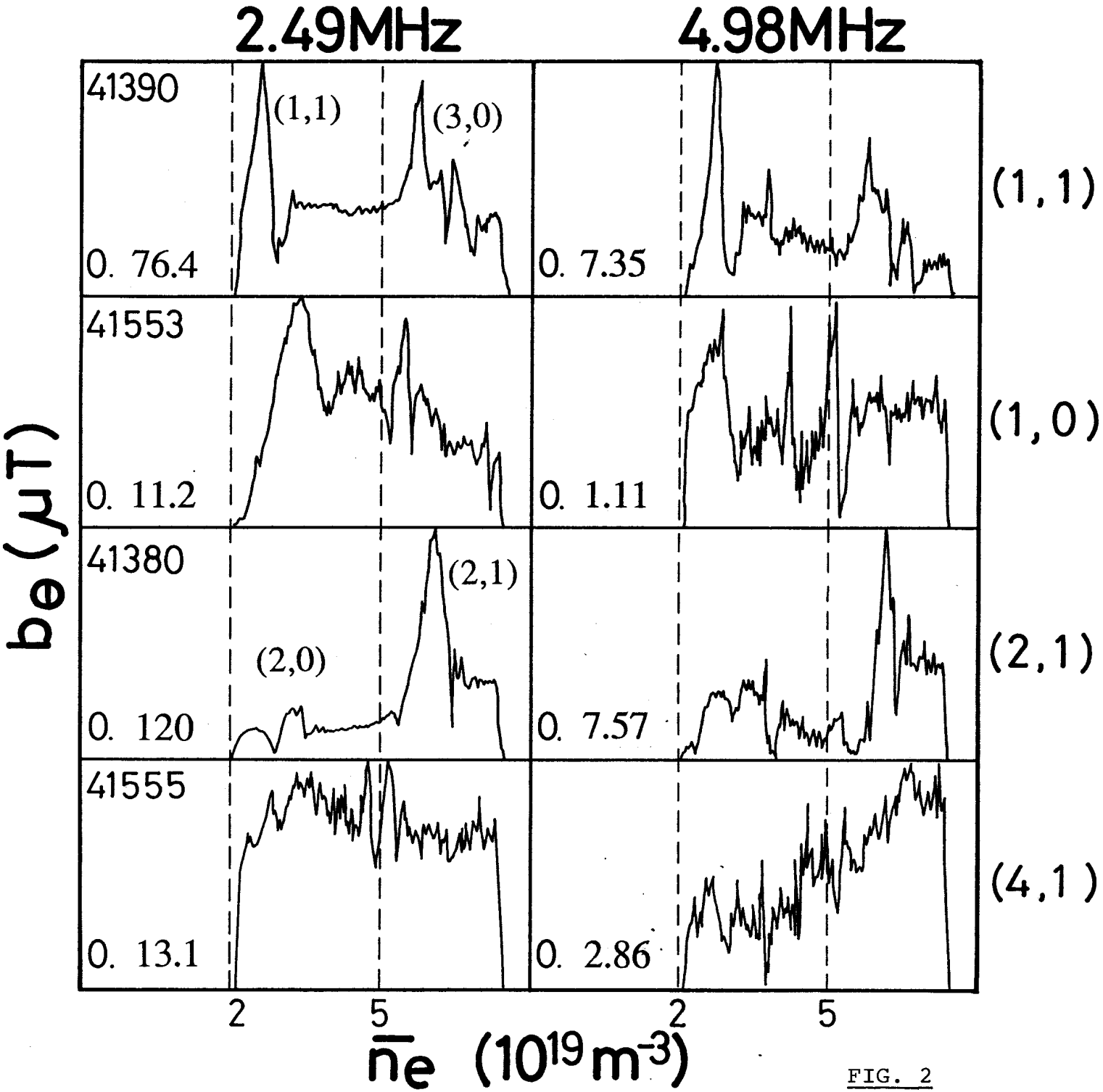
2.49MHz
4.98MHz
41390
(1,1)
(3,0)
0. 76.4
0. 7.35
(1,1)
41553
0. 11.2
0. 1.11
(1,0)
41380
(2,1)
(2,0)
0. 120
0. 7.57
(2,1)
41555
0. 13.1
0. 2.86
(4,1)
bθ (μT)
2
5
2
5
n̄e (10^19 m^-3)

FIG. 2

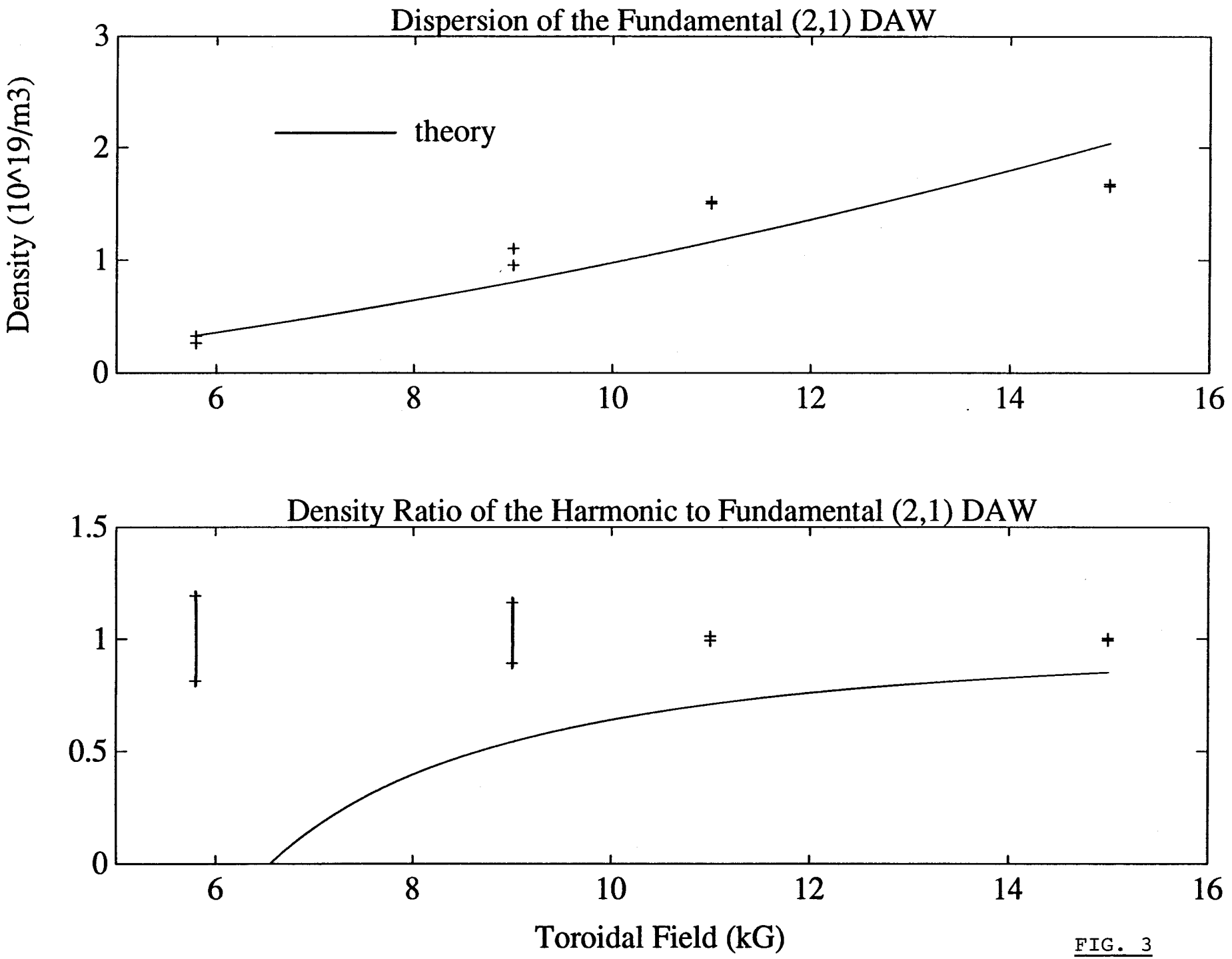
Dispersion of the Fundamental (2,1) DAW
Density (10^19/m3)
theory
3
2
1
0
6
8
10
12
14
16
Density Ratio of the Harmonic to Fundamental (2,1) DAW
1.5
1
0.5
0
6
8
10
12
14
16
Toroidal Field (kG)

FIG. 3

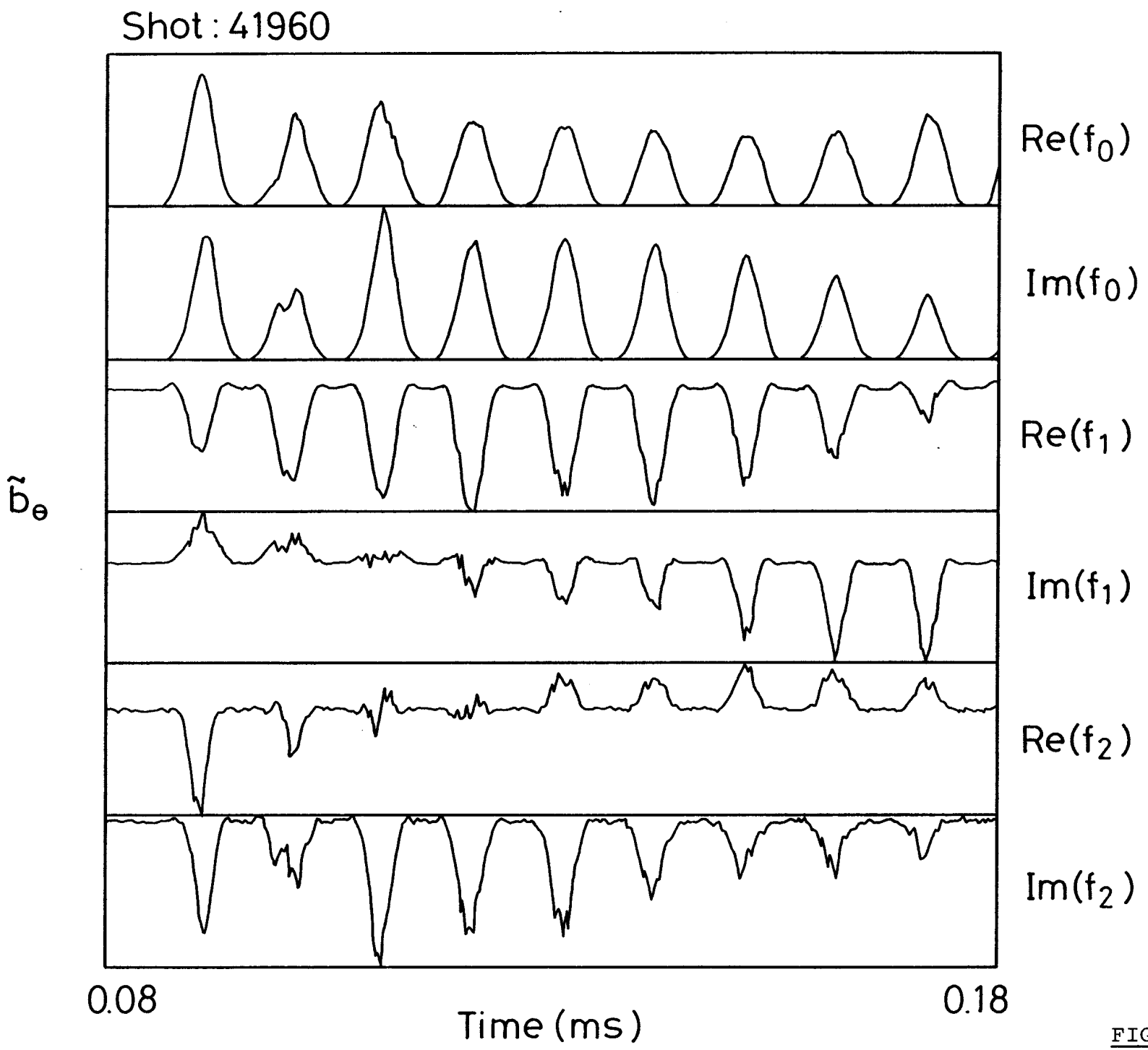

FIG. 4

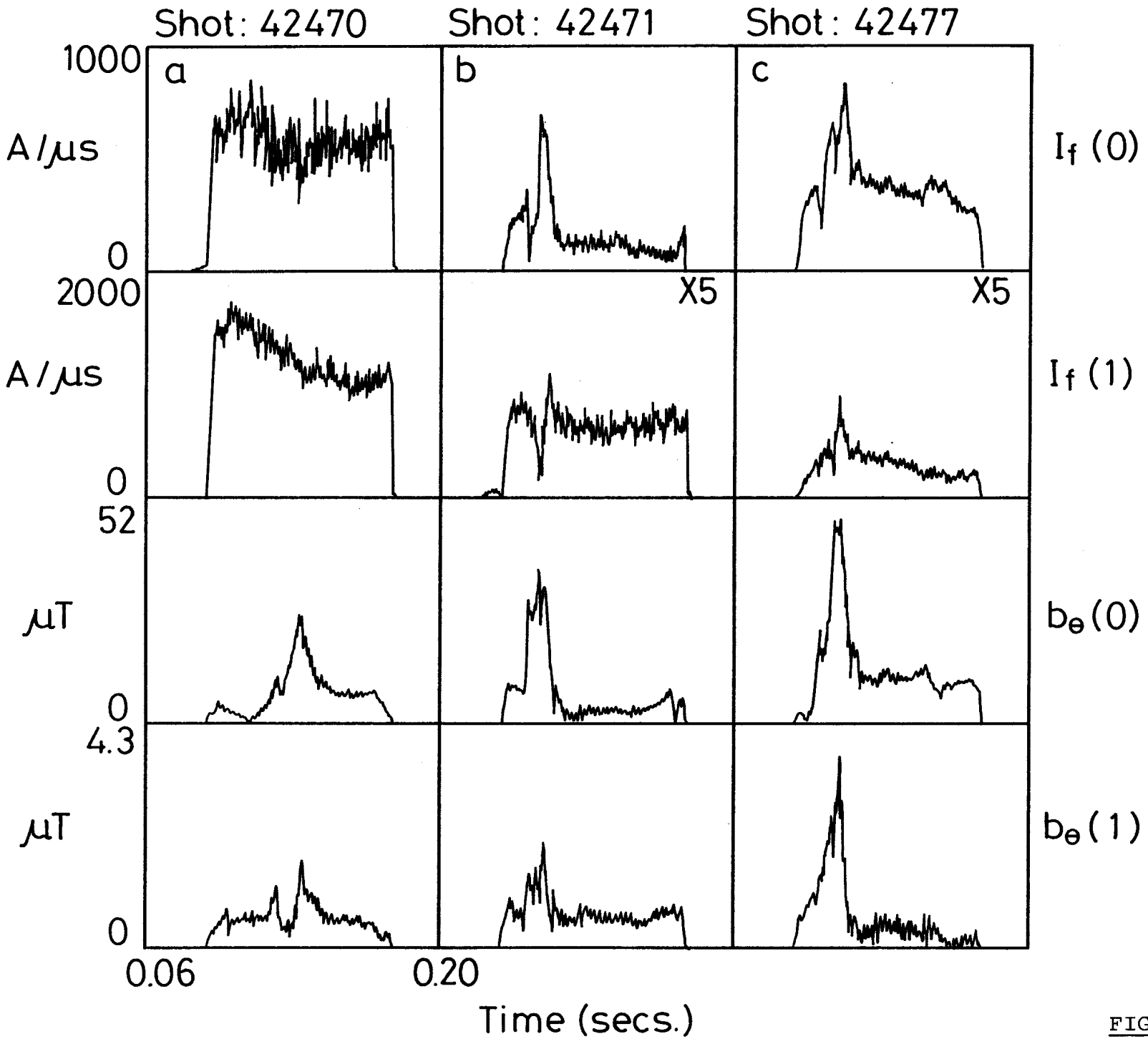
Shot: 42470
Shot: 42471
Shot: 42477
a
b
c
1000
A/μs
0
2000
A/μs
0
X5
X5
52
μT
0
4.3
μT
0
0.06
0.20
Time (secs.)
I_f (0)
I_f (1)
b_e (0)
b_e (1)

FIG. 5

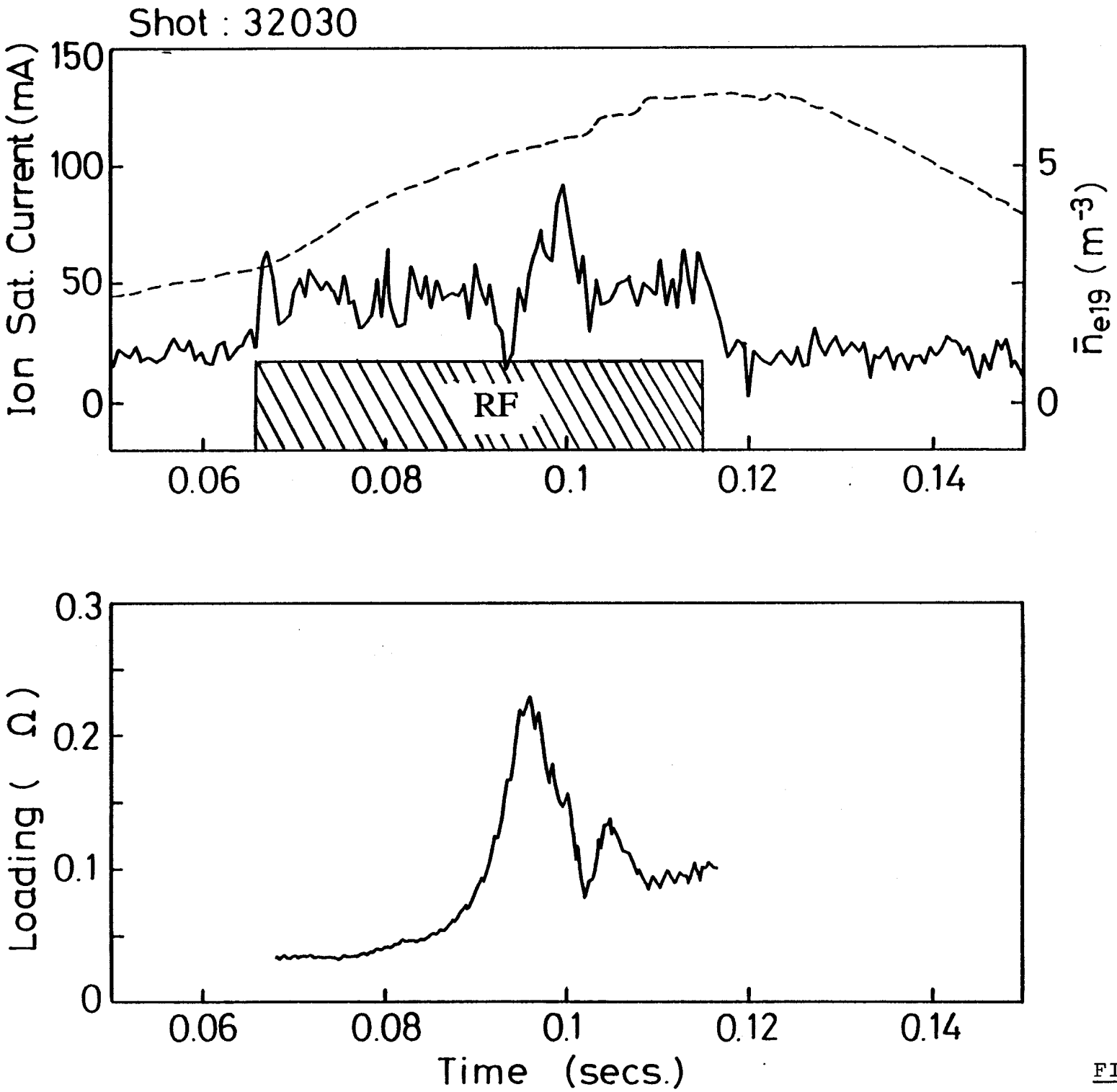
Shot : 32030
Ion Sat. Current (mA)
150
100
50
0
RF
$\bar{n}_{e19}$ (m^{-3})
5
0
0.06
0.08
0.1
0.12
0.14
Loading (Ω)
0.3
0.2
0.1
0
Time (secs.)

FIG. 6

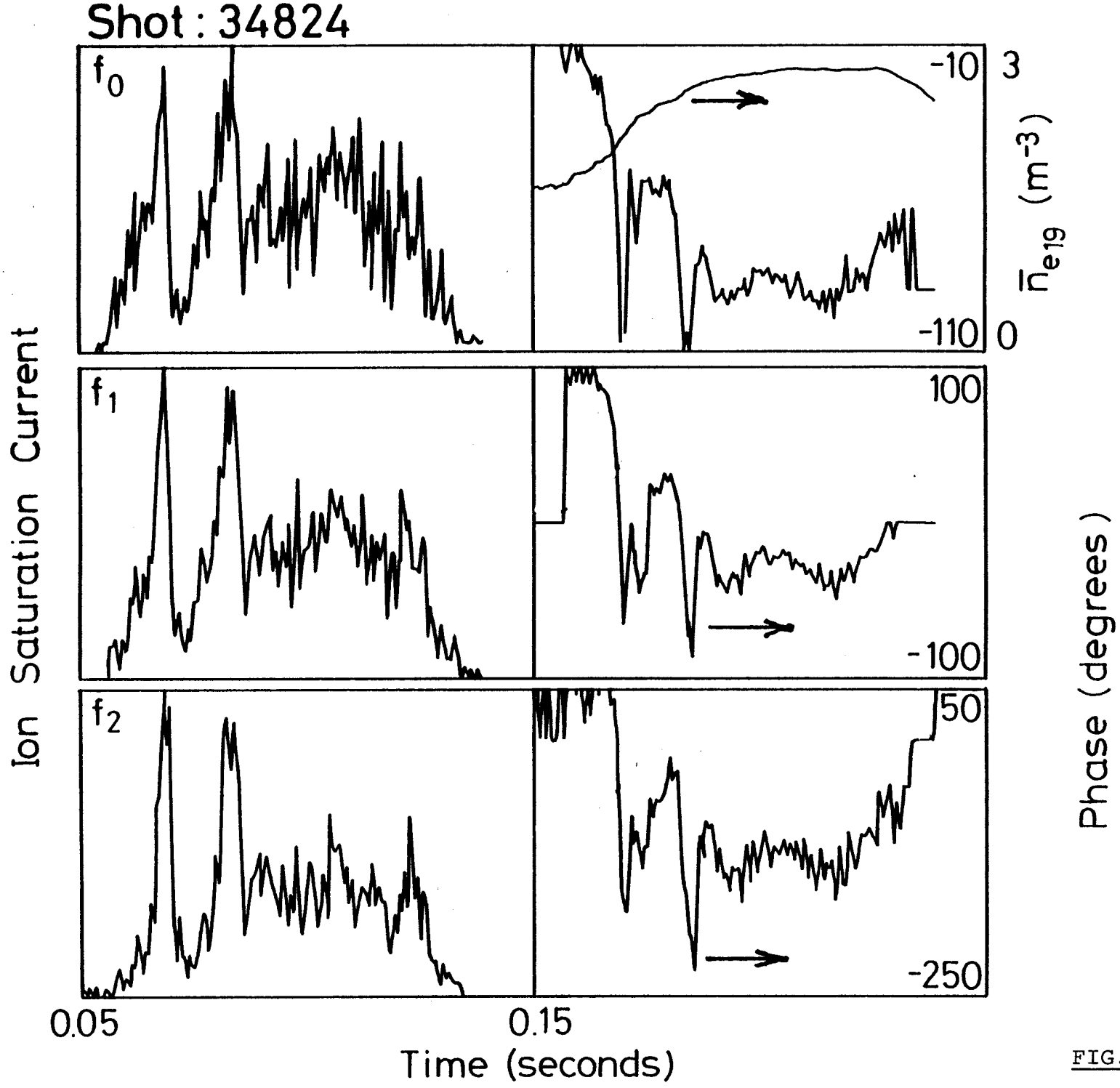
Shot : 34824
f_0
f_1
f_2
-10
-110
3
0
$\bar{n}_{e19}$ (m^{-3})
100
-100
50
-250
Ion Saturation Current
Phase (degrees)
0.05
0.15
Time (seconds)

FIG. 7

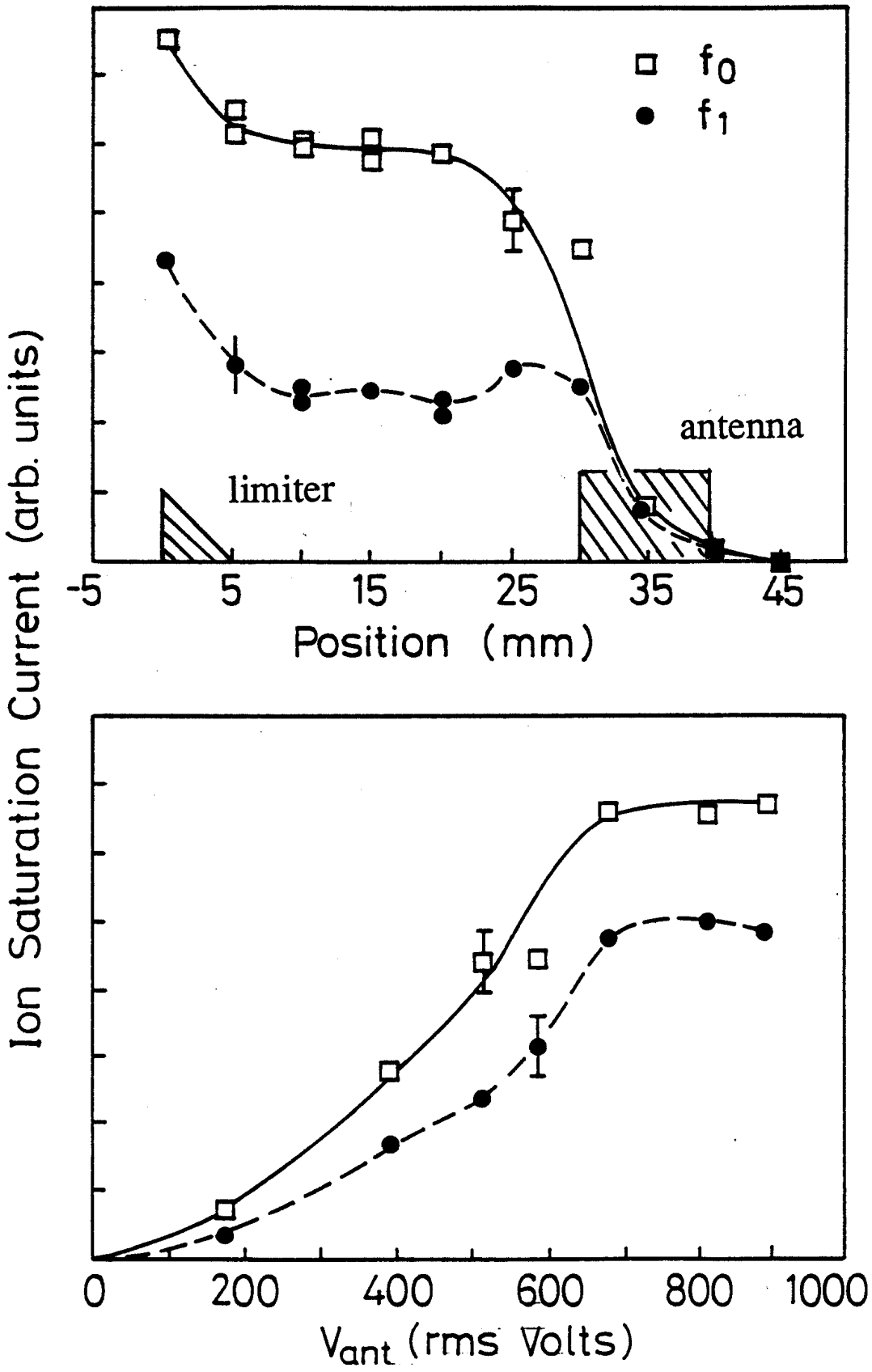
Ion Saturation Current (arb. units)
f_0
f_1
antenna
limiter
-5
5
15
25
35
45
Position (mm)
0
200
400
600
800
1000
V_{ant} (rms Volts)

FIG. 8